

Pre-irradiation induced grafting of styrene into crosslinked and non-crosslinked polytetrafluoroethylene films for polymer electrolyte fuel cell applications.

II: Characterization of the styrene grafted films

Jingye Li ^{a,*}, Kohei Sato ^a, Shogo Ichizuri ^a, Saneto Asano ^a, Shigetoshi Ikeda ^b, Minoru Iida ^b, Akihiro Oshima ^{a,b}, Yoneho Tabata ^{b,c}, Masakazu Washio ^{a,*}

^a Advanced Research Institute for Science and Engineering, Waseda University, 3-4-1, Okubo, Shinjuku, Tokyo 169-8555, Japan

^b RAYTECH Corporation, Sousyu Building 402, 4-40-13, Takadanobaba, Shinjuku, Tokyo 169-0075, Japan

^c Professor Emeritus, The University of Tokyo, 7-3-1, Hongo, Bunkyo, Tokyo 113-8656, Japan

Received 5 May 2004; received in revised form 4 October 2004; accepted 7 October 2004

Available online 16 December 2004

Abstract

Crosslinked and non-crosslinked polytetrafluoroethylene films (RX-PTFE and V-PTFE films, respectively) were irradiated by γ -ray and then grafted with styrene in liquid phase. Microscope FT-IR spectroscopy, TGA, solid state ^{13}C CP/MAS and high resolution HS/MAS NMR spectroscopy, wide-angle X-ray diffraction (WAXD) study were used to get the structural information of the styrene grafted RX-PTFE and V-PTFE films. From microscope FT-IR spectra of the grafted RX-PTFE films, the “grafting front mechanism” was proved. TGA analysis showed that the grafted films have a small degradation step and two main degradation steps. In the ^{13}C CP/MAS NMR spectra of the non-grafted films, there are no signal due to the absence of the hydrogen atom. While in the spectra of the grafted films, there are signals attributed to the polystyrene grafts. In the ^{13}C HS/MAS NMR spectra of the grafted films, the relative intensity of the peaks attributed to the polystyrene grafts increased while the relative intensity of the peak attributed to PTFE matrix decreased with the increase in the DOG. From WAXD patterns, the intensity of the crystalline peak decrease with the increase in the DOG. The grafted films were sulfonated by chlorosulfonic acid and the results of highest IEC value exceeded 3.0. Those results will be reported in the near future.

© 2004 Elsevier Ltd. All rights reserved.

Keywords: Polymer electrolyte fuel cell; Crosslinked and non-crosslinked polytetrafluoroethylene; Pre-irradiation induced graft polymerization; Structure characterization

1. Introduction

Polymer electrolyte fuel cells (PEFCs) are now in the focus as the most promising energy source for the vehicles and other mobile applications [1–3]. Proton exchange membranes (PEMs) are the important

* Corresponding authors. Tel.: +81 3 5286 2917; fax: +81 3 3205 0723.

E-mail addresses: jyli@waseda.jp (J. Li), washiom@waseda.jp (M. Washio).

component in the PEFCs, which separate the fuel gases and transport the protons [4]. Among the PEMs, Nafion® (Dupont de Nemours Ltd) membranes are the widely used. However, the high cost of the Nafion membranes encouraged the development of the cheaper and better fluorinated or non-fluorinated PEMs.

Radiation induced grafting of functional monomers into polymer films or membranes and successive sulfonation was designed as an alternative route to obtain the PEMs for PEFC applications [5,6, and the references cited]. Typically, styrene and co-monomers were grafted into the fluorinated polymer films or membranes and successive sulfonated to prepare the PEMs. Especially, the PEM obtained by grafting of styrene together with divinylbenzene (DVB) into FEP films and then sulfonation was reported to have a lifetime more than 10,000 h at 60 °C and 2500 h at 80 °C [7], which makes this method a promising way.

Several years ago, the crosslinked polytetrafluoroethylene (RX-PTFE) was developed by irradiation above the melting temperature of PTFE under oxygen-free atmosphere [8–11]. RX-PTFE showed remarkable improvements in several mechanical properties, radiation resistance, optical properties and so on, comparing with the non-crosslinked PTFE (V-PTFE) [12–14].

RX-PTFE holds a radiation resistant and chemical stable network structure, and the network structure can lower the gases permeation rate [15]. Thus it is a good candidate for the radiation induced grafting to prepare the PEMs.

Our research group is developing the fluoro-containing PEMs for PEFC applications by grafting of styrene into the RX-PTFE films under pre-irradiation method in gas [16] and liquid phase [17], and the V-PTFE films are also used as a reference. Previously, we have reported the kinetic study of the graft polymerization in liquid phase and some mechanical properties of the grafted films [17]. As a continuous work, in this paper we will report the study on the structure of the styrene grafted RX-PTFE and V-PTFE films which give important information on the grafting mechanism. Although there are many papers reported the characterization of the styrene grafted fluorinated films, the microscope FT-IR spectroscopy analysis and the solid state ^{13}C NMR spectroscopy analysis results were rarely reported. Therefore, we are devoted to give supplemental information of the structure of the grafted films for the better understanding of the graft polymerization mechanism and the effects of the reaction conditions on the grafted films.

2. Experiments

2.1. Materials

V-PTFE films of 0.5 mm thickness labeled as G-192 was obtained from Asahi Glass Fluoropolymers Co.

Ltd. (Japan). The molecular weight of V-PTFE was about 1.0×10^7 from the determination of heat of crystallization using Suwa's equation [18]. The RX-PTFE films were made of V-PTFE films by electron beam (EB) irradiation around 340 ± 5 °C under argon gas atmosphere, as described in our previous paper [10]. The RX-PTFE films used in this paper were crosslinked by irradiation with the dose of 100 kGy. The pre-irradiation induced grafting of styrene into RX-PTFE and V-PTFE films in liquid phase were described in our previous paper [17]. The degrees of grafting were determined as the weight increase of the samples according to the following equation:

Degree of grafting (DOG) (%)

$$= \frac{W_g - W_o}{W_o} \times 100\%, \quad (1)$$

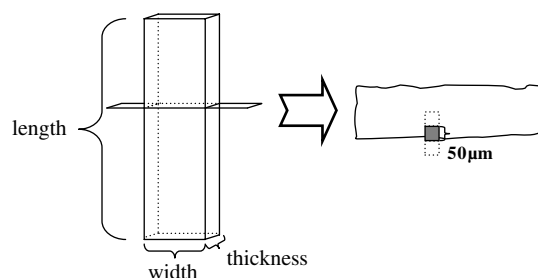
where W_g and W_o are the weights of the samples after and before grafting, respectively.

2.2. Measurements

The microscope FT-IR spectroscopy analyses were performed by a JIR-700 FT-IR instrument with an IR-MAU124 microscope unit, JEOL, Co., Ltd. (Japan). Samples were cut along the thickness direction and sliced samples with thickness of 50–100 μm were prepared. The IR beam was focused in a 50×50 μm area and the sliced samples were analyzed from one edge to the other with a step of 50 μm , which is shown in Scheme 1.

Thermogravimetric analysis (TGA) curves were recorded by a TGA 50H instrument, Shimadzu Co., Ltd. (Japan). The samples were heated from 50 to 750 °C at a heating speed of 5 °C/min under the nitrogen atmosphere.

Solid state ^{13}C cross-polarization (CP), magic angle spinning (MAS) NMR spectra were recorded with a JEOL CMX400 spectrometer operated at 100 MHz. The samples were rotated at a rate of 8 kHz at room temperature. CP spectra were acquired with a 3.1 μs proton 90° pulse and the contact time was 1ms. Typically



Scheme 1. The sampling method for the microscope FT-IR spectroscopy analysis.

700 transients were collected over a spectral width of 40 kHz.

Solid state high resolution ^{13}C high-speed (HS), magic angle spinning (MAS) NMR spectra were recorded with the same spectrometer as mentioned above. The samples were rotated at a rate of 5 kHz at 150 °C. Typically 700 transients were collected over a spectral width of 40 kHz.

Wide-angle X-ray diffraction (WAXD) patterns were performed by a RINT-1100 instrument, Rigaku Co., Ltd. (Japan) using Cu-K α irradiation. The voltage was set to 40 kV and the current was set to 20 mA. Data were collected at a rate of 2°min^{-1} with a step of 0.01° over the range of $2\theta = 5\text{--}50^\circ$.

3. Results and discussion

3.1. Microscope FT-IR spectroscopic analysis

Generally, the graft polymerization of the styrene only begins at the surfaces of the pre-irradiated RX-PTFE and V-PTFE films, and then penetrates into the interior, which was called “grafting front mechanism” [19–21]. In the matrices of the films, the interfaces between grafted and non-grafted base polymer was called “grafting fronts”. The moving rate of the grafting fronts is determined by the diffusion coefficient, the solubility of the polymer in the monomer, and so on. At certain reaction temperature, when the grafting period is long enough, the two grafting fronts will meet in the middle of the films and then disappear. For the applications in fuel cells, the films should be thoroughly grafted by styrene to achieve the bulk proton conductivity.

We use the step analysis by microscope FT-IR across the grafted films to observe the distribution of the PS grafts. The grafted films were cut along the thickness direction and thin slides with thickness of 50–100 μm were gotten as showed in Scheme 1. Only grafted RX-PTFE films were sampled, and the grafted V-PTFE films were too brittle to be cut into a thin slide. Then, the thin slides were mounted on the analysis holder. The FT-IR spectroscopy analyses were then performed from one edge of the slides to the other with a step of 50 μm and the FT-IR spectra across the films were gotten.

Fig. 1 shows the FT-IR spectra of the styrene grafted RX-PTFE film with DOG of 11%. The film was grafted at 60 °C for 2 h. From the spectra, it is observed that the two 100 μm slides from the surfaces were grafted by PS, where the bands which are attributed to the PS grafts and the RX-PTFE matrix all exist. The absorption bands are assigned according to the literature [14,22,23]. The bands from 3100 to 3000 cm^{-1} are the $=\text{C}\text{--}\text{H}$ stretching vibration of the PS grafts. The band at 2924 cm^{-1} is the asymmetric stretching and the band at 2849 cm^{-1} is the symmetric stretching of the aliphatic CH_2 group of the PS grafts. The bands at 1600 and 1583 cm^{-1} are the skeletal $\text{C}=\text{C}$ stretching vibration where the bands at 1492 and 1452 cm^{-1} are the skeletal $\text{C}=\text{C}$ in-plane deformation of the PS grafts. The bands from 1140 to 1267 cm^{-1} are the stretching vibration of CF_2 in the RX-PTFE matrix and the bands from 943 to 982 cm^{-1} are the stretching vibration of CF_3 in the RX-PTFE matrix. The band at 842 cm^{-1} is due to the aromatic out-of-plane $\text{C}\text{--}\text{H}$ deformation of the mono-substituted benzene ring. The intensities of the absorbance peaks are weak at the surface part due to the irregular of the film surface due to the grafting, thus

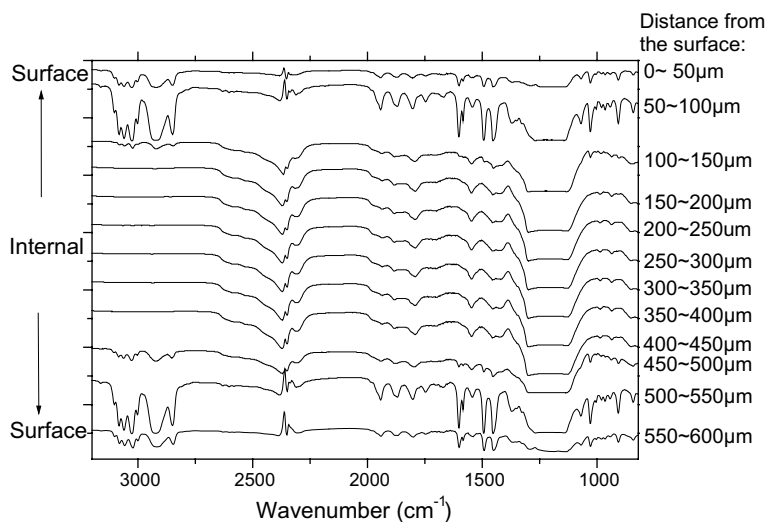


Fig. 1. FT-IR spectra of the styrene grafted RX-PTFE film across the thickness direction. DOG is 11%.

the analysis area is not fully covered by the samples to be analyzed.

In the matrix of the film, that is 150 μm from the both surfaces to the middle of the film, only the CF_2 and CF_3 signals of the RX-PTFE matrix are exist, and no signal of the PS grafts. It is obvious that there is no graft polymerization taken place. While in the slides of 100–150 μm from the both surfaces, there are weak signals of the PS grafts with strong signals of the RX-PTFE matrix. This means that the grafting fronts moved into about 100 μm from the both surfaces of the film in 2 h at 60 $^\circ\text{C}$.

FT-IR spectra of the styrene grafted RX-PTFE film with DOG of 39% are shown in Fig. 2. The film was grafted at 60 $^\circ\text{C}$ for 6 h. Similar to the case shown in Fig. 1, there are two grafting fronts at about 250 μm from the both surfaces of the film. From the surfaces to the grafting fronts, the RX-PTFE was grafted by styrene and there are signals attributed to both the RX-PTFE matrix and the PS grafts. Between two grafting fronts, the RX-PTFE was not grafted and there are only signals attributed to the PTFE chains.

FT-IR spectra of the styrene grafted RX-PTFE film with DOG of 91% are shown in Fig. 3. The film was grafted at 60 $^\circ\text{C}$ for 16 h. Different from the above cases, there are signals attributed to the PS grafts together with signals attributed to the RX-PTFE matrix across the film, no grafting fronts were found in the film. That means the grafting fronts met in the middle of the film and disappeared, and the film was grafted by styrene thoroughly. In such a case, the film is possible to be thoroughly sulfonated and to serve as the proton transporter.

The moving rate of the grafting fronts could be calculated by dividing the thickness of the grafted layers by

the reaction time under same reaction temperature. However, in our cases the step of 50 μm was used in the scanning, it was difficult to get the exact thickness of the grafted and non-grafted parts in the layer containing the grafting front. This will introduce large error in the calculation of the moving rate of the grafting fronts. Also, the irregular of the grafted surfaces of the films is another source for the possible error in calculation. Therefore, we did not calculate the moving rate of the grafting fronts as the error estimated may be over 10%.

3.2. Thermogravimetric analysis

Fig. 4 shows the TGA curves of non-grafted and grafted V-PTFE films. For the non-grafted V-PTFE film, it began to degrade at 490 $^\circ\text{C}$ and ended at 620 $^\circ\text{C}$ [14]. For the grafted V-PTFE films, there are mainly two separated steps degradation pattern in the TGA curves. The first degradation step began at 340 $^\circ\text{C}$ and ended at 425 $^\circ\text{C}$ and the second degradation step began at 490 $^\circ\text{C}$ and ended at 620 $^\circ\text{C}$. It is clearly that the first degradation step should be attributed to the degradation of PS grafts [24] and the second degradation step should be attributed to the degradation of the V-PTFE matrix. However, besides these two main degradation steps, there is a small degradation step from 130 to 235 $^\circ\text{C}$. Since the homopolymer was carefully washed off by hot solvent and the solvent was drove off by heated in vacuum as reported in our previous paper [17], this step of degradation should be attributed to the degradation of the random scissions due to the so called “weak links” in the backbone of the free-radical-initiated polystyrene as reported [25,26]. The weight percent of this degradation step increases with the increasing in the DOG. The weight percents of the small degradation step

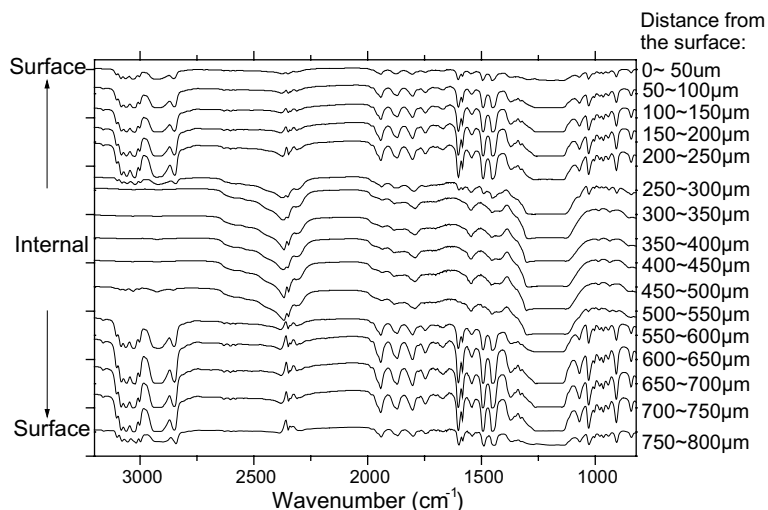


Fig. 2. FT-IR spectra of the styrene grafted RX-PTFE film across the thickness direction. DOG is 39%.

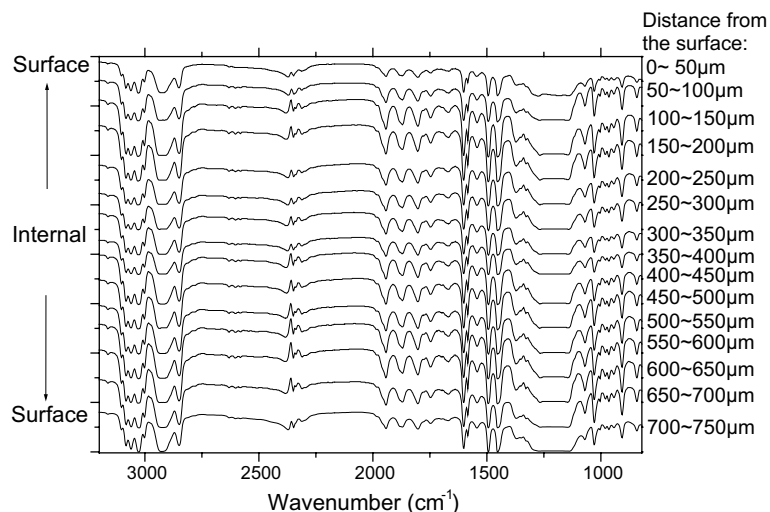


Fig. 3. FT-IR spectra of the styrene grafted RX-PTFE film across the thickness direction. DOG is 91%.

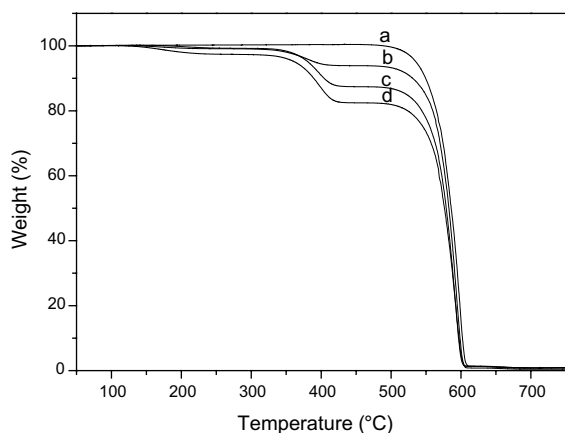


Fig. 4. TGA curves of (a) V-PTFE film and styrene grafted V-PTFE films with DOG of (b) 6%, (c) 15% and (d) 23%.

and two main degradation steps of non-grafted and grafted V-PTFE films are listed in Table 1.

Fig. 5 shows the TGA curves of non-grafted and grafted RX-PTFE films. For the non-grafted RX-PTFE film, it began to degrade at 420 °C and ended at 620 °C. The beginning temperature of the degradation of RX-

PTFE film is lower than that of V-PTFE film, which is due to the crosslinking under irradiation at high temperature which caused partial scission of PTFE chains and introduced unstable structure like double bonds [14]. For the grafted RX-PTFE films, there are mainly two continuous steps of degradation patterns in the TGA curves. The first degradation step began at 340 °C and ended around 420 °C and then second degradation step ended at 620 °C. It is considered that the first degradation step should be attributed to the degradation of PS grafts and the second degradation step should be attributed to the degradation of the RX-PTFE matrix but the end part of the first step was overlapped by the beginning part of the second step. Similar to the grafted V-PTFE films, there is a degradation step from 130 to 235 °C due to the degradation of the random scissions of the PS grafts. The weight percents of the small degradation step and two main degradation steps of the non-grafted and grafted RX-PTFE films are listed in Table 2.

3.3. Solid state ^{13}C NMR analysis

The solid state ^{13}C CP/MAS NMR spectra of the non-grafted and grafted RX-PTFE films are shown in

Table 1

The weight loss percents of the non-grafted and grafted V-PTFE films in the three degradation steps

DOG (%)	W_1 (%) (130–235 °C)	W_2 (%) (340–425 °C)	W_3 (%) (490–620 °C)
0	0	0	98.6
6	0.6	4.6	92.8
15	0.9	11.1	85.9
23	2.5	14.0	80.9

W_1 , W_2 and W_3 are the weight loss percent of the three degradation steps.

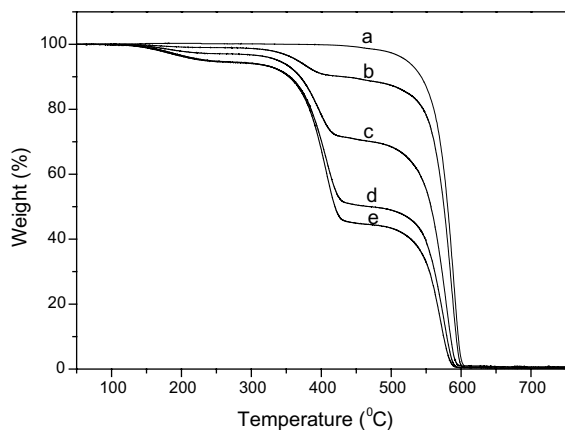


Fig. 5. TGA curves of (a) RX-PTFE film and styrene grafted RX-PTFE films with DOG of (b) 14%, (c) 39%, (d) 97% and (e) 133%.

Fig. 6. Due to the absence of the hydrogen atoms in the RX-PTFE chains, there are no signals of the non-grafted RX-PTFE under CP/MAS mode which is shown in Fig. 6(a). When styrene was grafted into RX-PTFE films, several peaks are appeared on the spectra as shown in Fig. 6(b)–(d). In the spectra of the grafted RX-PTFE films, all the signals are attributed to PS grafts and thus it is difficult to compare the component changing with different DOG by use RX-PTFE matrix as an inner reference. The attribution of the signals is according to Ref. [27]. In the spectra, the methylene and methine carbons of PS grafts have broad resonance frequencies at 42 ppm. The signal of aromatic carbons at 128 ppm and the signal of the quarterly carbon atom in the benzene ring at 147 ppm were also assigned to PS grafts. The methyl peak at 25 ppm was assigned to the end groups of the PS grafts. Due to the high intensity of the peak, it can be assumed that the number of PS chains is large and that the chain length of the PS grafts is relatively small. The peak intensities in CP/MAS spectra changed largely on the experimental parameters of the measurement, thus the estimation of the chain length of the PS grafts is still difficult. The shape of the spectra and the attribution of the peaks of the non-grafted and grafted V-PTFE films are similar to those of the non-grafted and grafted RX-PTFE films.

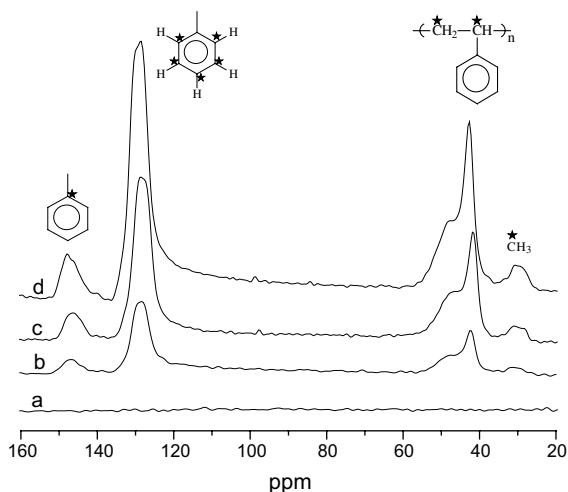


Fig. 6. Solid state ^{13}C CP/MAS NMR spectra of (a) RX-PTFE film and styrene grafted RX-PTFE films with DOG of (b) 14%, (c) 39% and (d) 97%.

As the above analysis did not show the component changing with the increase in DOG of the grafted films, we performed the solid state high resolution ^{13}C HS-MAS NMR analysis of non-grafted and grafted PTFE films. The ^{13}C HS-MAS NMR spectra of the non-grafted and grafted RX-PTFE films are shown in Fig. 7. In the spectrum of the non-grafted RX-PTFE film, there is only one peak at 110 ppm for the perfluoromethylene carbon [14]. After the grafting of styrene into RX-PTFE films, the peaks at 127 ppm for aromatic carbons, at 144 ppm for the quarterly carbon atom in the benzene ring and at 40 ppm for the methylene and methine carbons of PS grafts appeared [28]. The relative peak intensity is also changes with the increase in DOG. When the DOG is low, the perfluoromethylene carbon peak at 110 ppm is the main peak and there is only a small peak at 127 ppm stand for aromatic carbons. With the increase in DOG, the intensity of the peak at 127 ppm increased remarkably and is similar to that of the peak at 110 ppm. As the DOG further increased, the peak at 127 ppm became the main peak. From the spectra it is clear that the content of PS grafts in the grafted RX-PTFE films increased with the increase in DOG. In the solid

Table 2

The weight loss percents of the non-grafted and grafted RX-PTFE films in the three degradation steps

DOG (%)	W_1 (%) (130–235 °C)	W_2 (%) (340–420 °C)	W_3 (%) (420–620 °C)
0	0	0	98.8
14	1.0	8.3	89.9
39	2.7	24.3	71.2
97	4.8	38.5	54.9
133	4.6	44.2	49.1

W_1 , W_2 and W_3 are the weight loss percent of the three degradation steps.

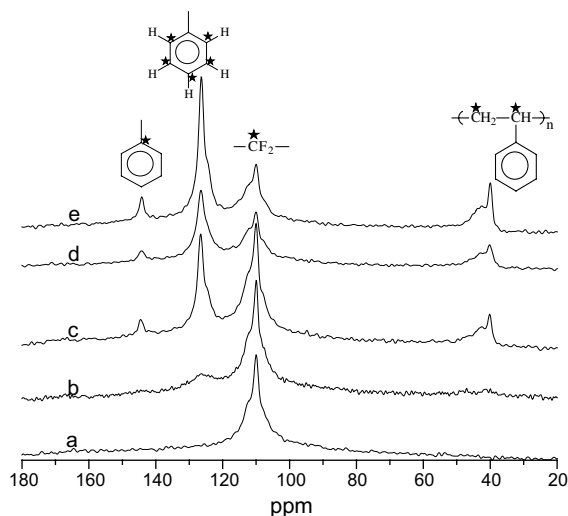


Fig. 7. High-resolution solid state ^{13}C HS-MAS NMR spectra of (a) RX-PTFE film and styrene grafted RX-PTFE films with DOG of (b) 14%, (c) 39%, (d) 97% and (e) 133%.

state ^{13}C HS-MAS NMR spectra of the non-grafted and grafted V-PTFE films, the intensity of the peaks attributed to PS grafts increased with the increase in DOG but the perfluoromethylene carbon peak still holds the strongest relative intensity due to the relatively low DOG. Since the sensitivity of the probe used in our instrument is not high enough, and there was no signal of the end groups of the PS grafts in the ^{13}C HS/MAS NMR spectra, therefore it is difficult to estimate the average chain length of the PS grafts.

3.4. WAXD diffraction measurement

WAXD patterns of the non-grafted and grafted V-PTFE films are shown in Fig. 8. It is obvious that the crystallinity peak for the non-grafted and all grafted V-PTFE films appears at the same angle, where 2θ equals to 18° . And there are the amorphous peak at 2θ equals to 16° . This means that there is no change in the structure after the grafting of styrene into V-PTFE films. However, the peak intensities of all grafted films are lower than that of non-grafted V-PTFE films, and the peak intensities are decreased with the increase in DOG. It was attributed to the dilution of the inherent crystallinity by the grafted amorphous PS grafts, as reported [22,29].

The diffraction patterns of the non-grafted and grafted RX-PTFE films, which are shown in Fig. 9, are similar to those of the V-PTFE films. Because of the reduction in the degree of crystallinity of the non-grafted RX-PTFE films, which was proved by DSC analysis [15], the signals of the non-grafted RX-PTFE films are much weaker than that of the non-grafted

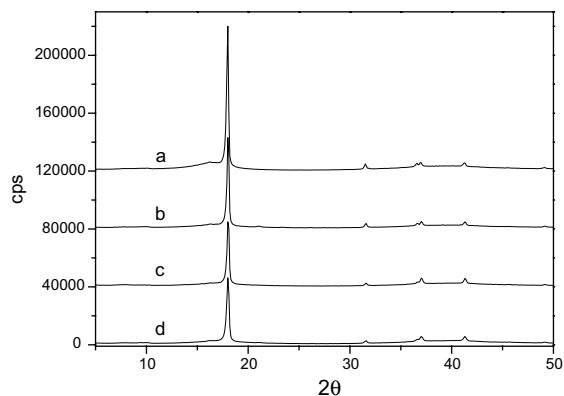


Fig. 8. Wide angle X-ray diffraction patterns of (a) V-PTFE film and styrene grafted V-PTFE films with DOG of (b) 6%, (c) 15% and (d) 23%.

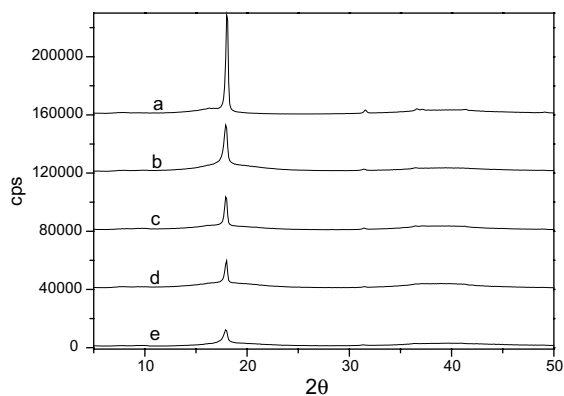


Fig. 9. Wide angle X-ray diffraction patterns of (a) RX-PTFE film and styrene grafted RX-PTFE films with DOG of (b) 14%, (c) 39%, (d) 97% and (e) 133%.

V-PTFE films. Also, the crystalline peak intensities of the grafted RX-PTFE films are decreased with the increase in DOG.

The degree of crystallinity was calculated from the WAXD data according to the following formula [30]:

Degree of crystallinity (DOC) (%)

$$= \frac{A_c}{A_c + A_a} \times 100\%, \quad (2)$$

where A_c is the area of the crystalline peak at 2θ equals to 18° , A_a is the area of the amorphous scattering part integrated in the range of $5^\circ \leq 2\theta \leq 30^\circ$.

As it was reported that the PTFE crystalline was diluted by the amorphous PS grafts [22,29], we calculated the expected degree of crystallinity only considering the dilution effect. The expected degree of crystallinity was calculated according to the following formula:

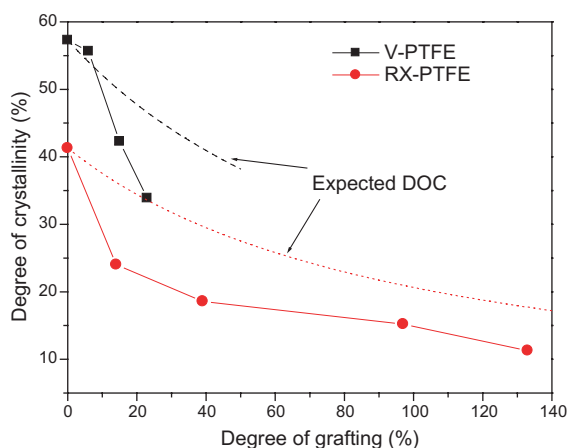


Fig. 10. The real and expected degree of crystallinity versus the degree of grafting of styrene grafted RX-PTFE and V-PTFE films.

$$\begin{aligned}
 \text{Expected DOC (\%)} &= \frac{W_c}{W_{\text{total}}} \times 100\% \\
 &= \frac{W_c}{W_{\text{PTFE}} + W_{\text{PS}}} \times 100\% \\
 &= \frac{\text{DOC}_{\text{non-grafted}}}{100 + \text{DOG}} \times 100\%, \quad (3)
 \end{aligned}$$

where $\text{DOC}_{\text{non-grafted}}$ are the DOC calculated from WAXD data of the V-PTFE and RX-PTFE before grafting.

Fig. 10 showed the real dependence of the DOC on the DOG and the expected curves. It was found that the real DOC decreased with the increase in DOG. But the decrease was quicker than the expected curves when the DOG was lower than 60%. When the DOG was higher than 60%, the DOC decreased very slowly and the tendency of the decrease is the same with the expected curves. This means that the dilution effect is the main reason for the decrease in the DOC when the DOG is high. But when the DOG is low, there should be weak crystalline decomposition happened besides the dilution effect. In the pre-irradiation procedure, there were radicals appeared not only in the amorphous domain but also in the crystalline domain of the PTFE. Therefore, there was graft polymerization taken place in the crystalline domain thus some crystalline decomposed. This may be the reason besides the extent of phase segregation of PS and PTFE segments account for the dramatic lost in the mechanical strength of the grafted films as we reported in previous work [17].

4. Conclusion

Crosslinked and non-crosslinked polytetrafluoroethylene films (RX-PTFE and V-PTFE films, respectively) were irradiated by γ -ray to 30 kGy in air and then

grafted with styrene in liquid phase. Microscope FT-IR spectroscopic study was carried out to get the distribution of the polystyrene (PS) grafts in RX-PTFE films and the “grafting front mechanism” was proved. For grafted RX-PTFE film with DOG of 11%, two 100 μm slides from surfaces were grafted by styrene and the middle of the film there was not grafted. That means the grafting fronts moved into about 100 μm from both surfaces of the film. In the grafted RX-PTFE film with DOG of 39%, there are two grafting fronts at about 250 μm from both surfaces of the film. In the grafted RX-PTFE film with DOG of 91%, it was grafted by styrene thoroughly and no grafting fronts were observed in the matrix. TGA analysis showed that the non-grafted V-PTFE film has one degradation step. While the grafted V-PTFE films have a small degradation step of the random scission in the PS grafts and two main separated degradation steps of the PS grafts and PTFE matrix. The grafted RX-PTFE films have the similar three degradation steps pattern. In the solid state ^{13}C CP/MAS NMR spectra of the non-grafted films there are no signal due to the absence of the hydrogen atom while in the spectra of the grafted films there are signals attributed to the PS grafts. In the solid state high resolution ^{13}C HS/MAS NMR spectra of the grafted films, the relative intensity of the peaks attributed to the PS grafts increased while the intensity of the peak attributed to the PTFE matrix decreased with the increase in DOG, which indicated the increase in the content of the PS grafts with the increase in DOG. From WAXD patterns of the non-grafted and grafted films, the grafting of styrene into the films did not change the crystalline structure of the PTFE matrix but diluted the concentration of the crystalline zone. The degree of crystallinity was calculated, and it decreased with the increase in DOG. When the DOG is low, the decrease is due to some crystalline decomposition by grafting and the dilution by amorphous PS grafts. When the DOG is high, the decrease is mainly due to the dilution effect.

The grafted films were sulfonated by chlorosulfonic acid and the electrical properties and the chemical structure of the sulfonated films are now in analysis. The highest IEC value of the PEMs gained exceeded 3.0.

Acknowledgement

The authors acknowledge Prof. Y. Katsumura and Dr. C. Matsuura for γ -ray irradiation experiments and various discussions. The authors also acknowledge Prof. Y. Hama and research associate Dr. T. Oka for FT-IR experiments. The development of the new PEM using RX-PTFE was supported by projects of “Research and Development of Polymer Electrolyte Fuel Cell” in

the New Energy and Industrial Technology Development Organization (NEDO).

References

- [1] Acres GJK. *J Power Source* 2001;100:60–6.
- [2] Stambouli BA, Traversa E. *Renew Sust Energy Rev* 2002;6:295–304.
- [3] Hall J, Kerr R. *J Cleaner Prod* 2003;11:459–71.
- [4] Mehta V, Cooper JS. *J Power Source* 2003;114:32–53.
- [5] Dargaville TR, George GA, Hill DJT, Whittaker AK. *Prog Polym Sci* 2003;28:1355–76.
- [6] Nasef MM, Hegasy EA. *Prog Polym Sci* 2004;29:499–561.
- [7] Huslage H, Brack H-P, Geiger F, Büchi FN, Tsukada A, Scherer GG. *PSI Scientific Report* 1998, Annex V, 1999. p. 51–2.
- [8] Oshima A, Tabata Y, Seguchi T. In: *Proceedings of 14th International Symposium on Florin Chemistry*, Yokohama, Japan, July, 1994.
- [9] Sun J, Zhang Y, Zhong X, Zhu X. *Radiat Phys Chem* 1994;44:655.
- [10] Oshima A, Tabata Y, Kudoh H, Seguchi T. *Radiat Phys Chem* 1995;45:269–73.
- [11] Tabata Y, Oshima A, Takashika K, Seguchi T. *Radiat Phys Chem* 1996;48:563–8.
- [12] Oshima A, Ikeda S, Kudoh H, Seguchi T, Tabata Y. *Radiat Phys Chem* 1997;50:611–5.
- [13] Tabata Y, Oshima A. *Macromol Symp* 1999;143:337–58.
- [14] Oshima A, Ikeda S, Katoh E, Tabata Y. *Radiat Phys Chem* 2001;62:39–45.
- [15] Oshima A, Seguchi T, Tabata Y. *Radiat Phys Chem* 1999;55:61–71.
- [16] Sato K, Ikeda S, Iida M, Oshima A, Tabata Y, Washio M. *Nucl Instr Meth Phys Res B* 2003;208:424–8.
- [17] Li JY, Sato K, Ichizuri S, Asano S, Ikeda S, Iida M, et al. *Eur Polym J* 2004;40:775–83.
- [18] Suwa T, Takehisa M, Machi S. *J Appl Polym Sci* 1973;17:3253–7.
- [19] Gupta B, Büchi FN, Scherer GG. *J Polym Sci Part A* 1995;33:1545–9.
- [20] Gupta B, Büchi FN, Staub M, Grman D, Scherer GG. *J Polym Sci Part A* 1996;34:1873–80.
- [21] Brack H-P, Scherer GG. *Macromol Symp* 1997;126:25–49.
- [22] Nasef MM, Saidi H, Dessouki AM, El-Nesr EM. *Polym Int* 2000;49:399–406.
- [23] Cutler DJ, Hendra PJ, Rahalkar RR, Cudby MEA. *Polymer* 1981;22:726–30.
- [24] Cardona F, Hill DJT, George G, Maeji J, Firas R, Perera S. *Polym Degrad Stab* 2001;74:219–27.
- [25] Chiantore O, Camino G, Costa L. *Polym Degrad Stab* 1981;3:209–19.
- [26] Mark HF, Bikales NM, Overberger CG, Menges G, Kroschwitz JI, editor. *Encyclopedia of polymer science and engineering*, vol. 16. New York: John Wiley & Sons Inc.; 1989. p. 180–4.
- [27] Hietala S, Maunu SL, Sundholm F. *Macromolecules* 1999;32:788–91.
- [28] Yamamoto Y, Amutharani D, Sivakumar M, Tsujita Y, Yoshimizu H. *Desalination* 2002;148:289–91.
- [29] Nasef MM, Saidi H, Nor HM. *J Appl Polym Sci* 2000;76:220–7.
- [30] Abdou SM, Mohamed RI. *J Phys Chem Solids* 2002;63:393–8.